catalysts

MDPI

Article

Integrated Photocatalytic Oxidation and Adsorption Approach for the Robust Treatment of Refinery Wastewater Using Hybrid TiO_2/AC

Ihtisham Ul Haq [1], Waqas Ahmad [1,*], Imtiaz Ahmad [1,*], Amjad Shah [2], Muhammad Yaseen [1] and Taj Muhammad [1]

[1] Institute of Chemical Sciences, University of Peshawar, Peshawar 25120, Khyber Pakhtunkhwa, Pakistan
[2] School of Energy and Electronic Engineering, University of Portsmouth, Portsmouth PO1 2UP, UK
* Correspondence: waqasahmad@uop.edu.pk (W.A.); patwar2001@yahoo.co.in (I.A.)

Abstract: This study reports the removal of hydrocarbon (HC) pollutants from petroleum refinery wastewater by integrated photocatalytic oxidation and adsorption using a TiO_2/AC hybrid material. The hybrid adsorbent/catalyst was prepared by the impregnation of TiO_2 over AC and characterized by FTIR, SEM, EDX, and XRD analyses. Under the optimized reaction conditions of pH 3, 30 °C, and 1000 mg TiO_2/AC per 500 mL of sample in 50 min, the integrated photocatalytic oxidation-adsorption achieved a net percentage removal of benzene, toluene, aniline, and naphthalene of 91% from model HC solutions. Under these conditions, for the treatment of real refinery wastewater, TiO_2/AC caused a 95% decrease in chemical oxygen demand (COD). The integrated photocatalytic oxidation and adsorption using TiO_2/AC showed a clear advantage over the individual adsorption and photocatalytic oxidation using AC and TiO_2, whereby about the same level of removal of model HCs and a decrease in the COD of refinery wastewater was attained in 105 min and 90 min, respectively, utilizing larger adsorbent/catalyst dosages. GC-MS analysis revealed that during the integrated process of adsorption-photocatalytic oxidation, all the parent HCs and oxidation byproducts were completely removed from the refinery wastewater. Based on the outstanding performance, cost-effectiveness, and environmental greenness, the newly designed TiO_2/AC via the integrated adsorption-photocatalytic oxidation can be counted as an effective alternative route for the large-scale processing of refinery wastewater.

Keywords: refinery wastewater; hydrocarbon pollutants; photocatalytic oxidation; adsorption; activated carbon; chemical oxygen demand

Citation: Ul Haq, I.; Ahmad, W.; Ahmad, I.; Shah, A.; Yaseen, M.; Muhammad, T. Integrated Photocatalytic Oxidation and Adsorption Approach for the Robust Treatment of Refinery Wastewater Using Hybrid TiO_2/AC. *Catalysts* **2023**, *13*, 193. https://doi.org/10.3390/catal13010193

Academic Editors: Sheng Guo, Yazi Liu and Jun Li

Received: 17 December 2022
Revised: 7 January 2023
Accepted: 10 January 2023
Published: 13 January 2023

1. Introduction

A large amount of oily wastewater is produced in the petroleum industry from the upstream production of crude oil to its storage, which eventually flows downstream from transportation and then refining processes [1,2]. Recently, many efforts have been devoted to minimizing the waste produced during crude oil refining, which largely consists of different types of petroleum hydrocarbons (HCs) [3–5] (Table 1). Due to the excessive requirements and the usage of water in oil refineries at various stages, a significant quantity of wastewater (0.4–0.6 times that of the crude oil refined) is produced that is laden with different levels of HC pollutants [6,7]. More seriously, the global requirement for crude oil is on the rise [8]; hence, the production of petroleum wastewater is also increasing. The toxic HC-laden wastewater not only contributes to atmospheric pollution through the escape of volatiles, but it also creates soil and water pollution [9]. With climate change and increased environmental awareness, the practice of venting off refinery wastewater in large quantities is becoming increasingly unacceptable without the necessary treatment. Several efforts have been documented to develop efficient techniques for treating such wastewater, including biodegradation, pyrolysis, photocatalysis, ultrasonic treatments, adsorption, solvent

extraction, land farming, incineration, and advanced oxidation processes [5,10–13]. With these techniques, the toxic components can be minimized to a certain level; however, their complete removal is not yet possible due to the recalcitrant nature of HCs, which necessitates the development of new and more advanced techniques to ensure public health [12].

Table 1. Typical composition of refinery wastewater.

pH	Level (mg/L)							Ref.
	BOD	COD	SS	O&G	Phenols	NH_3	$-SO_4^{-2}$	
7–9	150–360	300–600	≤150	≤50	-	15	-	[14]
8.0	40.25	80–120	22.8	-	13	-	-	[15]
6.6	-	596	120	-	-	-	887	[16]
	150–350	300–800	100	3000	20–300	-	-	[17]
8.0	570	850–1020	-	12.7	98–128	5.1–2.11	15–23	[18]
10	8.0	80.8	-	47.5	-	2.3	-	[17]
	-	658–710.5	-	45	30	22	10	[19]

Adsorption treatment of oily wastewater is preferred due to its low cost, simplicity of operation, recycling of adsorbent material, and easy applicability. The adsorbents used for the removal of HC pollutants can be classified into three classes, i.e., inorganic mineral adsorbents such as clays, silica, zeolite, etc. [20]; organic synthetic adsorbents, such as polymers, polymer composites, or polyurethane foams, etc. [21]; and bio adsorbents, including agricultural residues, corn cob, straws, saw dust, etc., which are all low-cost materials but offer poor efficiency [22]. Among these, mineral clays constitute an important class of natural aluminosilicates that are widely used for the removal of different wastewater contaminants because of their low cost, high surface area, and high adsorption performance [23]. Due to the hydrophilic nature of the clays, they are generally not suitable for the adsorption of aliphatic and aromatic HCs present in the oil-contaminated wastewater [24]. In order to make them organophilic, the natural clays are modified with various surfactants, by which the cationic and anionic sites of the clay matrix are exchanged with organic cations or anions [25]. The most common adsorbent used for the removal of organic waste and HCs from wastewater is activated carbon (AC) [26]. AC derived from coconut shell was reported to remove 90% of chemical oxygen demand (COD) from refinery wastewater [27]. Similarly, activated coke obtained from lignite achieved a 53% reduction in COD from heavy oil wastewater [28]. Okiel and his team [29] reported promising results for the removal of HCs from an oil–water emulsion using powdered AC (PAC), deposited carbon (DC), and bentonite as adsorbents. However, AC provides limited efficiency in the case of high concentrations of organic pollutants.

Catalytic photochemical oxidation has become popular because of its simple operation, versatility, and high efficiency in the removal of a wide variety of organic pollutants from wastewater [30,31]. In this process, the HCs in water are converted into harmless H_2O and CO_2 via the generation of a highly reactive (2.8 V oxidation potential) hydroxyl radical (OH.) in the presence of a photocatalyst and UV radiation. The distinct feature of the OH. radical is a wide range of selectivity and high oxidation activity, and hence, it can facilitate the oxidation of refinery wastewater laden with HCs [32–34]. In the photocatalytic degradation of organics, oxides of various semiconductors such as SnO_2, WO_3, CeO_2, Fe_2O_3, ZnO, ZnS, CdS, SiO_2, and TiO_2 have been reported to be efficient photocatalysts [10,35]. Among these, TiO_2 has earned a vital position for the oxidation of HCs in wastewater due to its high efficiency, stability, easy availability, low cost, and convenient recovery from the treated wastewater [36,37]. In this regard, a UV/TiO_2 oxidation system has shown high activity in the degradation of a wide range of organic pollutants [35,38], and it has also proved to be a good choice for the degradation of HCs in refinery wastewater. However, this approach suffers from high processing costs and the continued existence of some oxidation products in the treated wastewater [39,40].

Inspired by previous reports, this study reports the removal of HC pollutants from petroleum refinery wastewater by integrated photocatalytic oxidation-adsorption techniques using a TiO_2/AC hybrid adsorbent/catalyst. The hybrid material was synthesized by impregnating TiO_2 over AC, and it was characterized by scanning electron microscopy (SEM), energy dispersive X-ray (EDX) analysis, X-ray diffraction (XRD), and Fourier transform infra-red (FTIR) spectroscopy. The removal of HC pollutants was investigated using model as well real refinery wastewater samples in a specially designed photoreactor. The HC removed from the treated refinery waste was monitored through high-performance liquid chromatography (HPLC), COD analysis, and gas chromatography mass–spectrometry (GC-MS) analyses.

2. Results and Discussion

2.1. Characterization of TiO_2/AC Hybrid Adsorbent

The chemical composition of TiO_2/AC was characterized by FT-IR, and the results are shown in Figure 1. AC exhibited low-intensity peaks at 3400 cm^{-1} that show O-H of the carboxyl group and a peak at 1700 that shows the presence of C=O groups indicating carbonyl or carboxylic configurations. Peaks positioned around 1600 cm^{-1} indicate C=C functionalities of aromatics. The FTIR spectra of TiO_2/AC show characteristics peaks of AC, in addition to a strong absorption peak at 500 cm^{-1} that is ascribed to the vibration of Ti-O bonds in the TiO_2 lattice [41]. These results affirm the preparation of the TiO_2/AC hybrid adsorbent material.

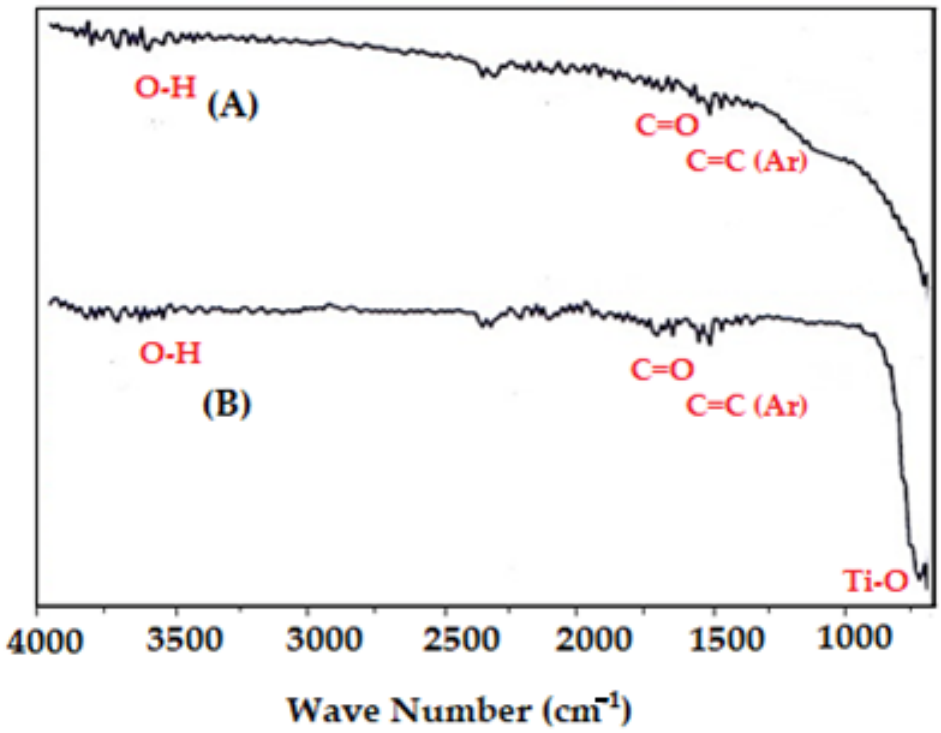

Figure 1. FTIR spectra of (A) AC and (B) TiO_2/AC.

SEM characterizes the surface monological features, particles shape, and distribution, and hence, the AC and TiO_2/AC hybrid materials were studied by SEM. The SEM micrograph of the AC (Figure 2a) shows a rough, heterogenous, and uneven surface, with some surface layers folded out in the form of dispersed flakes. The surface seems highly porous and spongy, which may show good adsorption behavior. The SEM micrograph of TiO_2/AC (Figure 2b) also shows similar morphology as that of the AC; however, distinct crystallites of TiO_2 (bright spots) can be seen dispersed on the surface of the AC, which evidence the incorporation of TiO_2 on the surface of the AC. The elemental composition of the TiO_2/AC

hybrid adsorbent was analyzed by EDX analysis. The EDX profile is shown in Figure S1 (Supplementary Materials), and the percentage weights of the various elements are given in Table 2. The data show that the TiO_2/AC contains high percentages of C, O, and Ti, which are about 66, 28, and 2%, respectively. However, some other elements, such as Al, Si, S, Ca, and Zn, were also found to be present in minor quantities, which may be assumed to be associated with matrix of the AC.

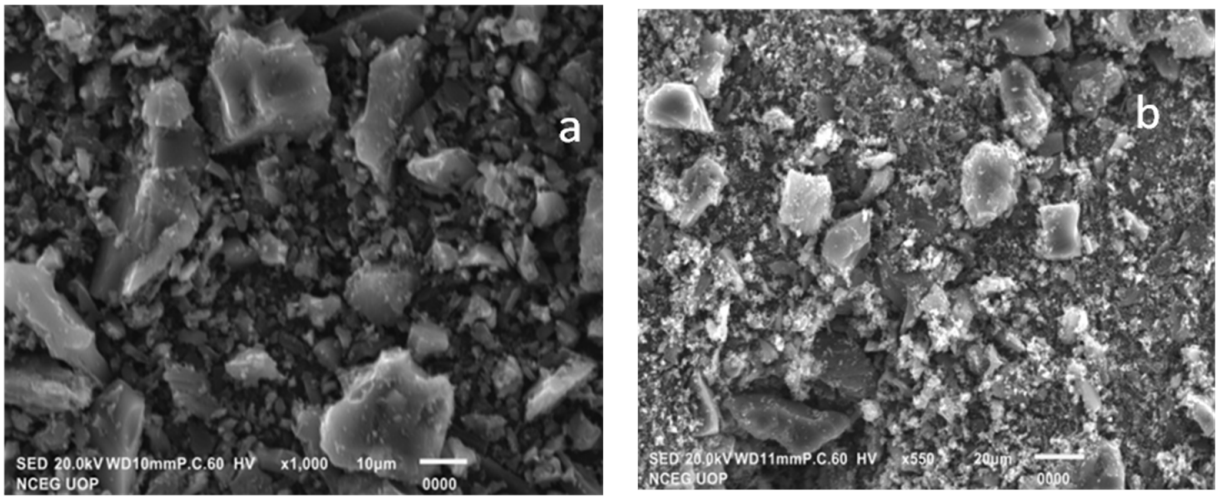

Figure 2. SEM micrographs of (**a**) AC and (**b**) TiO_2/AC.

Table 2. Elemental composition of TiO_2/AC.

Elements	Mass %	Elements	Mass %
C	66.65	Al	0.38
O	28.71	Si	0.72
Ti	2.0	S	0.12
Ca	0.90	Zn	0.53

The XRD patterns of the AC and TiO_2/AC are shown in Figure 3. The XRD pattern of AC shows a typical amorphous pattern with an intense peak at around 2θ of 24.3°, which can be assigned to the graphite configuration [42]. The XRD pattern of the TiO_2/AC shows the characteristics peaks corresponding to the rutile phase at 2θ of 27, 36, and 55 [43], as well as the anatase phase at 2θ of 25 and 48, which match with the standard cards of JCPDS 88-1175 and JCPDS 84-1286, respectively [44]. This confirms the successful impregnation of TiO_2 over the AC surface.

2.2. Adsorption over AC

The adsorption of HC pollutants from model and refinery wastewater was studied using AC in batch mode experiments. Initial adsorption experiments were carried out with model wastewater under conditions of different temperatures, adsorption times, and adsorbent doses to find the optimum conditions required for the maximum removal of HCs.

The adsorption experiments of 100 mL model wastewater were carried out at an ambient temperature for 60 min using different weights of AC as adsorbent dosages ranging from 100 mg to 800 mg. The results are shown in Figure 4, which indicate that the percentage removal of all model HCs linearly increased with an increase in the adsorbent dose up to 600 mg, beyond which no increase in percentage removal occurs. The maximum removal of benzene, toluene, phenol, and naphthalene was 55, 46, 45, and 49%, respectively, at an AC dose of 600 mg. However, with a further rise in the AC dose, the percentage removal of HC remained constant. The adsorption of organic substances over the surface of the AC commonly occurs via Van der Waals forces or π–π interaction [17]. The increase in adsorption of HCs at higher AC doses is due to more availability of vacant adsorption

sites on the surface of the AC. Under low AC doses, the level of adsorption is low because of insufficient reactive sites for adsorption, which increases with an increasing AC dose. In the case of a higher adsorbent dose, the abundance of adsorbents may aggregate, which constrains the accessibility of free surface for adsorption [45].

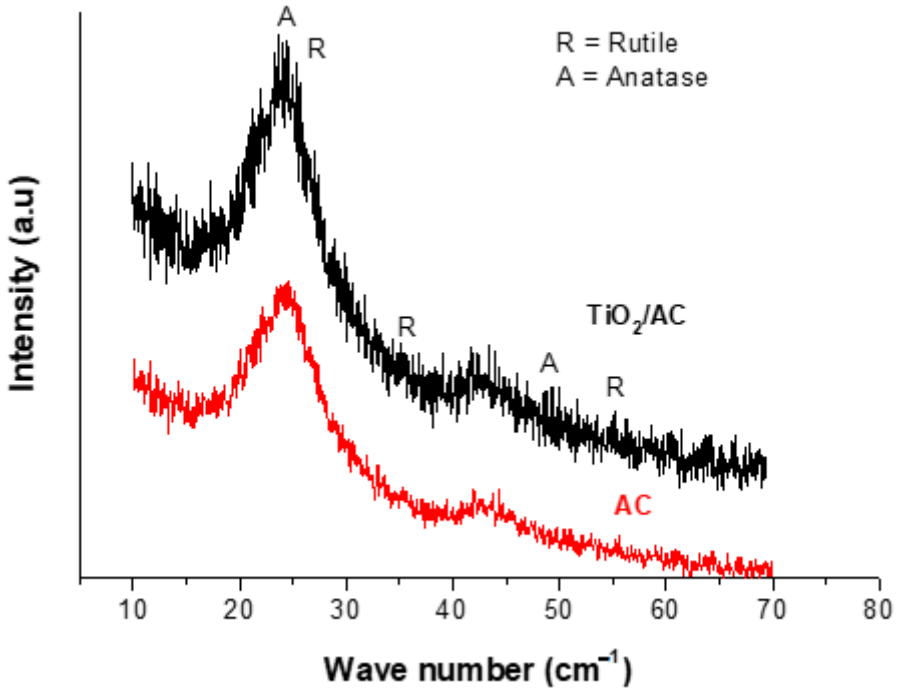

Figure 3. XRD Pattern of AC and TiO_2/AC.

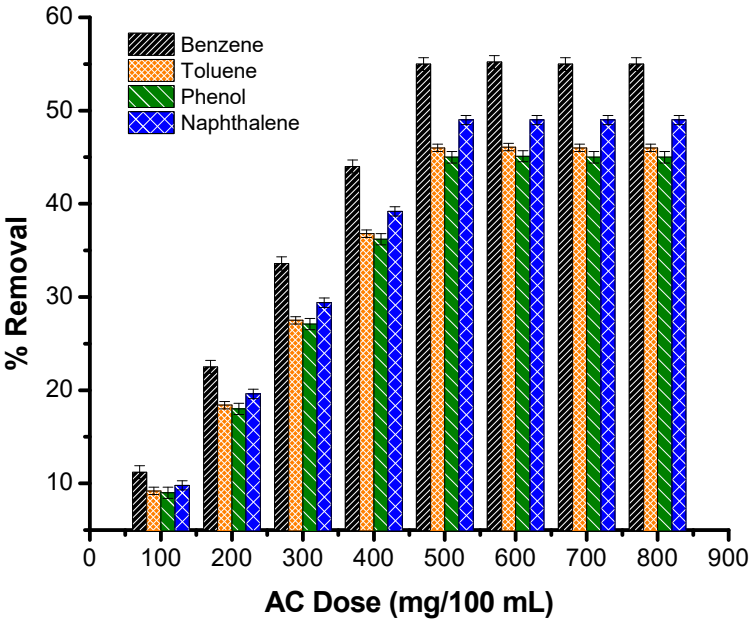

Figure 4. Effect of AC dosage on the removal of HCs from model wastewater (ambient temperature, 60 min, feed volume 100 mL).

The adsorption of HCs under various temperatures, i.e., 30, 35, 40, 45, and 50 °C, shows that (Figure 5) the removal of HCs from the model wastewater increases by a factor of 10% with an increase in temperature from 30 to 35 °C. However, with a further increase in temperature from 40 to 50 °C, no positive influence is observed; rather, the adsorption of all model HCs slightly declines at a higher temperature. This may be attributed to the

weakening of the electrostatic attraction between the HC molecules and the surface of the AC at higher temperatures, which in turn leads to a decrease in the level of adsorption [46].

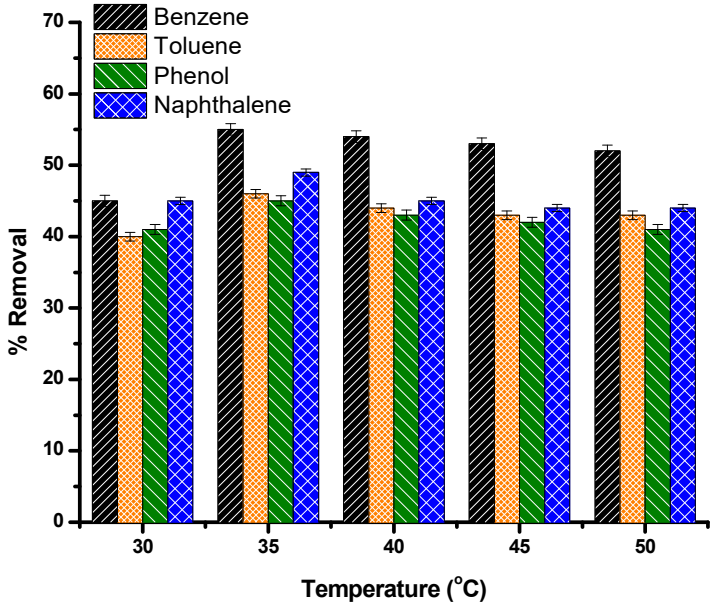

Figure 5. Effect of temperature on the removal of HCs from model wastewater using AC (60 min, adsorbent dose 600 mg/100 mL model wastewater).

The influence of adsorption time on the percentage removal of model HCs on the AC was investigated at different adsorption times, i.e., 15, 30, 45, 60, 75, 90, 105, 120, and 135 min. The results in Figure 6 indicate that the adsorption of HCs linearly rises with the increase in adsorption time and reaches a maximum of above 94% in 105 min; however, with a further increase in time, there is no increase in adsorption. These results suggest that initially, the adsorption rate increases with an increase in the adsorption time due to the availability of vacant adsorption sites on the surface of the AC, but as the vacant sites are occupied in 105 min, the adsorption then becomes constant [47]. The optimization of the adsorption time is important in controlling the cost of the process [17].

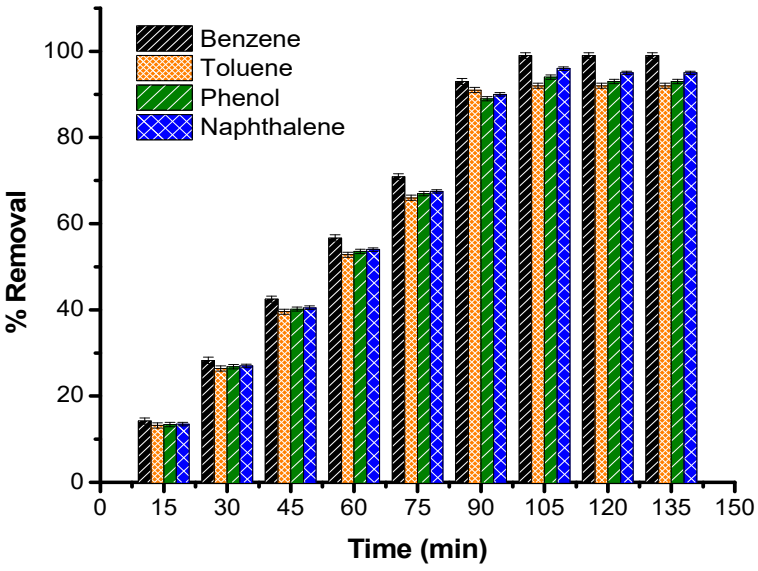

Figure 6. Effect of reaction time on the removal of HCs over AC from model wastewater (35 °C, adsorbent dose 600 mg/100 mL model wastewater).

2.3. Adsorption Kinetics

In order to investigate the mechanism of adsorption of model HC over AC, the pseudo-first-order and pseudo-second-order kinetics models were applied to the adsorption data. Figures S1 and S2 (Supplementary Materials) show the pseudo-first- and pseudo-second-order kinetic plots for the adsorption of benzene, toluene, phenol, and naphthalene over AC, whereas the values of rate constants, i.e., k_1, k_2, and the equilibrium concentration (q_e) and corresponding correlation coefficients are given in Table 3.

Table 3. Kinetic parameters for adsorption of model HCs on AC.

	Benzene	**Toluene**	**Phenol**	**Naphthalene**
Pseudo-first-order kinetic parameters				
k_1 (mg $g^{-1}min^{-1}$)	0.021	0.021	0.021	0.021
q_{e1} (mg g^{-1})	2.761	2.576	2.600	2.612
R^2	0.930	0.931	0.930	0.933
Pseudo-second-order kinetic parameters				
k_2 (mg $g^{-1}min^{-1}$)	0.044	0.024	0.025	0.017
q_{e2} (mg g^{-1})	4.878	3.676	3.760	0.067
R^2	0.150	0.101	0.179	0.261

The data show that, applying the pseudo-first-order kinetic model, the plots of $\ln(q_e - q_t)$ vs. time (t) for all the model HCs give linear plots with a R^2 of above 0.930 for all model compounds. Meanwhile, in the case of pseudo-second-order kinetics, non-linear plots are obtained from (t/q_t) vs. time (t) with a R^2 less than 0.261. This confirms that the pseudo-first-order kinetic model shows satisfactory correlation for the adsorption of HC onto AC. The current results agree with the reported literature, which shows that the adsorption of organic pollutants (acid blue dye) from water on AC prepared from waste rubber follows pseudo-first-order kinetics [48]. Similarly, other studies have also shown that the adsorption of benzene, toluene, and phenol over chemical AC agree with pseudo-first-order kinetics [49,50]. These results show that the adsorption of HCs over AC occurs through the liquid phase transport rate, rather than the intraparticle transport rate.

2.4. Adsorption Isotherms

The equilibrium data of adsorption were analyzed by adsorption isotherm models, which give important information about the interaction of the adsorbate and adsorbent. The Freundlich and Langmuir isotherm models were used to interpret the adsorption data. The Langmuir isotherm considers the monolayer adsorption on uniform adsorption sites, whereas the Freundlich isotherm explains multilayer adsorption on a heterogenous surface [51]. Figures S3 and S4 (Supplementary Materials) show the plots of the Langmuir and Freundlich isotherms for the adsorption of model HCs over AC, respectively. The Langmuir constants (K_1 and q_m) and Freundlich constants (n and K_f) calculated from the respective plots and the coefficients of correlation (R^2) for both isotherms are given in Table 4. The values of R^2 are close to 1 for both isotherms, which means that the adsorption data fit both the Langmuir and Freundlich isotherm models. This agrees with several studies, in which the adsorption of different adsorbates over various carbonaceous adsorbents follows both these adsorption isotherms [52–55]. This suggests that both chemical and physical adsorption is involved for the removal of HCs from the model wastewater. However, the adsorption of some HC pollutants, such as Benzene, phenol, toluene, etc., from water over AC derived from difference biomass sources follows the Langmuir adsorption isotherm [49,56]; on the other hand, the adsorption of similar compounds on variously activated AC samples follows the Freundlich isotherm [50,57].

Table 4. Isotherm parameters for adsorption of model HCs on AC.

Parameters	Benzene	Toluene	Phenol	Naphthalene
Langmuir isotherm parameters				
q_m (mg/g)	4.902	3.676	3.690	4.329
K_1	0.040	0.031	0.031	0.035
R^2	0.998	0.997	0.998	0.998
Freundlich isotherm parameters				
N	0.988	0.752	0.753	0.873
K_f	1.834	2.018	2.017	1.915
R^2	0.997	0.998	0.999	0.999

2.5. Thermodynamic Parameters

Various thermodynamic parameters, such as ΔG°, ΔH°, and ΔS°, were calculated from the adsorption data, and the results are shown in Table 5. It is clear that ΔH° shows negative values, which suggests the exothermic nature of the adsorption of benzene, toluene, phenol, and naphthalene onto AC, and this also affirms the results of the effect of temperature on the level of adsorption (Section 2.2). The positive values of ΔG° show that the adsorption and desorption are not in mutual thermodynamic equilibrium. An increase in the ΔG° value also indicates that the degree of spontaneity is higher at a lower temperature. The positive value of ΔS° shows that randomness increases at the solid liquid interface during adsorption, which may be associated with some changes in the structures of the adsorbent or adsorbate [58].

Table 5. Thermodynamic parameters for adsorption of model HCs on AC.

Temperature (°C)	ΔG° (kJ·mol^{-1})	ΔH° (kJ·mol^{-1})	ΔS° (kJ·mol^{-1})	ΔG° (kJ·mol^{-1})	ΔH° (kJ·mol^{-1})	ΔS° (kJ·mol^{-1})
	Benzene			Toluene		
30	4.560			5.076		
35	3.607			4.532		
40	3.771	−0.0010	0.002	4.816	−0.0004	0.001
45	3.937			5.000		
50	4.107			5.079		
	Phenol			Naphthalene		
30	4.971			4.556		
35	4.635			4.224		
40	4.922	−0.0017	0.001	4.710	−0.0007	0.001
45	5.101			4.893		
50	5.299			4.970		

2.6. Simultaneous Oxidation and Adsorption with TiO_2/AC

The removal of model HCs was investigated by simultaneous oxidation and adsorption over a TiO_2/AC hybrid material. Simultaneous oxidation and adsorption experiments were carried out in a photoreactor under UV irradiation at a temperature of 35 °C, a pH of 3, and 1 h contact time using different weights of TiO_2/AC ranging from 100 to 800 mg for 100 mL of a model wastewater sample. The results are shown in Figure 7, which indicate that the percentage removal of all the model HCs increased linearly with the increase in weight of the TiO_2/AC until 500 mg, beyond which the percentage removal became constant. Statistical analysis also confirmed the significant differences among model waste HCs, their doses, as well as their interaction (Table 6). Among the model waste HCs, the maximum percentage reduction of benzene occurred (59.97%), followed by phenol (58.31%), toluene (57.83%), and naphthalene (57.17%) at all doses. However, the maximum percentage removal of benzene (94.4%), toluene (92.7%), phenol (91%), and naphthalene (92%)

was attained at 500 mg TiO_2/AC (Table 7). With the increase in the weight of TiO_2/AC, the concentration of both the photocatalyst i.e., TiO_2, and the adsorbent, i.e., AC, increased; hence, the rate of photocatalytic oxidation and adsorption also increased.

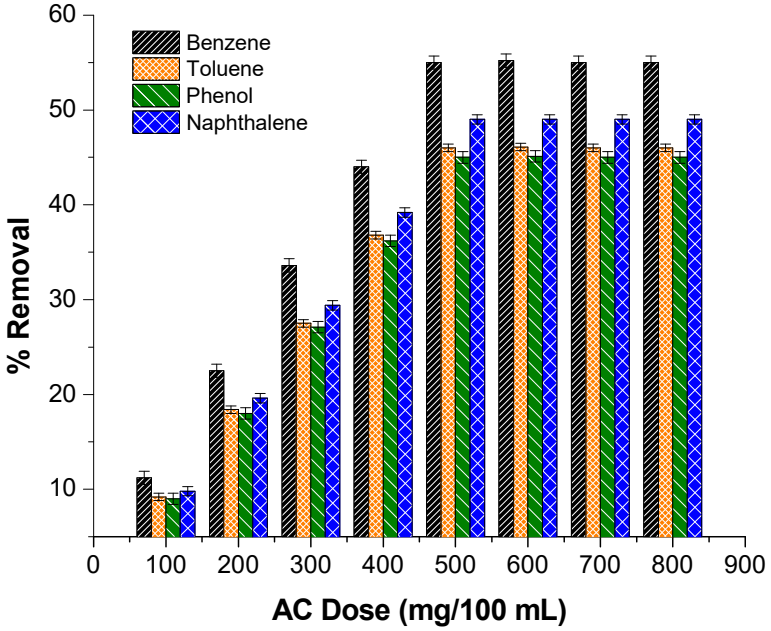

Figure 7. Effect of catalyst/adsorbent dose (TiO_2/AC) on removal of HC (35 °C temperature, pH 3, and 1 h contact time; feed volume 100 mL).

Table 6. Analysis of variance for % reduction of model waste by TiO_2/AC.

Sources of Variation	Df	Sum of Squares	Mean Square	F-Value	Prob. Value
Rep.	2	0.54136	0.27068		
Pollutants	3	140.275	46.7583	826.99 **	0.000
Error I	6	0.33924	0.05654		
Doses	10	104558	10455.8	307,591 **	0.000
Pollutant x Dose	30	149.635	4.98751	146.72 **	0.000
Error-II	80	2.71939	0.03399		
Total	131	104851			

** = Highly significant at $p \leq 0.05$ level of probability.

Table 7. Comparison test of TiO_2/AC dose vs. reduction in pollutant concentration.

Dose	Benzene	Toluene	Phenol	Naphthalene	Mean
100	10.500i	10.433i	11.100h	10.667i	10.675K
200	23.433f	21.700g	23.299f	21.500g	22.458J
300	33.167b	30.700d	32.333c	29.6333e	31.458I
400	42.700X	40.167Z	42.233Y	39.267a	41.092H
500	51.300T	49.333V	50.400U	48.300W	49.833G
600	59.200R	58.333S	60.367Q	58.267S	59.042F
700	70.233N	69.333O	69.300O	67.567P	69.108E
800	88.567J	81.233K	80.600L	79.300M	82.425D
900	92.133D	90.200H	89.733I	90.600G	90.667C
1000	94.400A	92.700C	91.033F	92.100D	92.233B
1100	94.00B	92.033DF	91.133F	91.767E	92.558A
Mean across all doses	59.967A	57.833C	58.312B	57.179D	

In order to examine the influence of reaction time on the process efficiency, simultaneous oxidation and adsorption experiments were carried out at different reaction times ranging from 10 to 80 min with 10 min increments. The results are shown in Figure 8, which indicate that the percentage removal of HCs was rapid up to 50 min, when the

maximum removal of all model HCs (average 92%) was attained, and then it remained constant. As mentioned above, about 90 % removal of HCs in the model wastewater was attained in 90 min in the case of simple photocatalytic oxidation using TiO_2, as well as in simple adsorption over AC separately, whereas the same level of removal occurred in 60 min in simultaneous oxidation and adsorption using TiO_2/AC. This shows the enhanced efficiency of the simultaneous process.

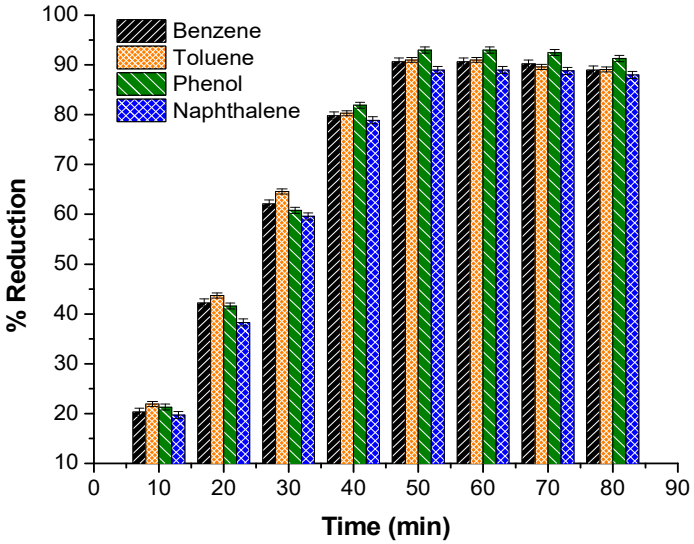

Figure 8. Effect of time on removal of HC using TiO_2/AC (35 °C temperature, pH 3, and 1 h contact time; TiO_2/AC dose 500 mg/100 mL feed volume).

Our previous lab experiments showed that in the case of simple photocatalytic oxidation using 100 mg of a TiO_2 catalyst, the maximum percentage removal of benzene, toluene, phenol, and naphthalene in 60 min was about 43.5, 42.1, 45.8, and 44.6% respectively [40]. Likewise, in the present study, the maximum removal of benzene, toluene, phenol, and naphthalene by simple adsorption using 500 mg AC was about 55, 46, 45, and 49% respectively, in 60 min. On the other hand, in the case of integrated photocatalytic oxidation and adsorption, using 500 mg of TiO_2/AC, above 90% removal of the same model HCs was attained in 50 min reaction time. These results clearly show the advantage of the integrated treatment process over the individual photocatalytic oxidation and adsorption.

2.7. Treatment of Refinery Wastewater

Refinery wastewater samples were collected from the Attock Oil Refinery in Rawalpindi, Pakistan. Samples were collected at the point at which wastewater leaves the dissolved air flotation (DAF) unit. The initial characterization of refinery wastewater, shown in Table S1 (Supplementary Materials), indicates that the values of various parameters such as the pH, turbidity, dissolved and suspended solids, and COD are beyond the permissible levels of the environmental health safety guidelines (2009). In particular, the pH and COD of the sample are critically high, i.e., 9.2 and 970 mg/L, versus the allowable limits [59,60]. Thus, the refinery wastewater sample requires proper treatment before being discharged into the environment.

The removal of HC pollutants from the refinery wastewater samples was investigated by simple adsorption over AC, photocatalytic oxidation using a UV/TiO_2 system, and integrated oxidation and adsorption over TiO_2/AC, and the results are presented in Table 8. The adsorption experiments were carried out in batch mode under optimized conditions, i.e., an AC dose of 600 mg/100 mL, 35 °C, and 105 min, respectively. The results indicate that the COD of the refinery wastewater was reduced to 77 mg/L after adsorption on the AC, thus attaining a significant reduction of about 92% in the COD. Likewise, in the case of photocatalytic oxidation over the UV/TiO_2 system under optimized conditions in our

previous study [40], i.e., pH 3, at 30 °C, in 90 min reaction time, and 100 mg/L catalyst dose, the COD of the refinery wastewater decreased to about 77 mg/L, thus attaining about a 93% decrease in COD.

Table 8. Decrease in COD of refinery wastewater by various treatment process.

Treatment of Refinery Wastewater	Reaction Time (min)	COD (mg/L)	Reduction in COD (%)
Untreated sample	-	970	-
Adsorption over AC	105	77	92
Photocatalytic oxidation by UV/TiO_2	90	65	93
Integrated photocatalytic oxidation and adsorption over TiO_2/AC	50	48.5	95

In the case of the integrated photocatalytic oxidation and adsorption process in the presence of TiO_2/AC at 30 °C temperature, 50 min treatment time, and using a 1000 mg/500 mL dose, there was a prominent reduction in the COD of the refinery wastewater, i.e., from 970 mg/L to 48.5 mg/L, accounting for about a 95% reduction in COD. These results clearly show the advantage of the integrated process using TiO_2/AC over the simple adsorption and photocatalytic oxidation. The integrated process brings about more than the same level of decrease in the COD of the refinery wastewater in just 50 min, which is attained by adsorption over AC in 105 min and photocatalytic oxidation using the UV/TiO_2 system in 90 min.

It may be inferred from the above results that the level of COD removed from the refinery wastewater with the current process is higher than the literature reports. For example, El-Gawad reported about a 79% removal of COD from wastewater, with initial COD values of 500 mg/L in 60 min adsorption time, using AC entrapped in alginate polymer [61]. A 45% and 40% reduction in COD was reported by Sun et al. in the case of coking and papermaking wastewater by adsorption over bottom ash, using a 10 g/100 mL waste sample [62]. Similarly, the COD removal attained through photocatalytic oxidation under different conditions has been found to be 63% [63], 78% [63], and 80% [64]. Thus, TiO_2/AC can potentially be used for the largescale treatment of refinery wastewater.

2.8. GC-MS Analysis

The GC-MS chromatograms of the refinery wastewater as collected from the source and the sample processed through adsorption over AC, photocatalytic oxidation over TiO_2, and integrated oxidation and adsorption over TiO_2/AC are displayed in Figure 9, and the types of HCs identified in each sample along with their retention times and relative percentage concentrations are given in Table S2 (Supplementary Materials). The GC-MS data showed that in the refinery wastewater sample, the concentration of aliphatic, aromatics, oxygenates, and naphthenic HCs was about 69.23, 25.36, 3.2, and 2.21 %, respectively. Among the aliphatic HCs, the major compounds occurring in the sample ranged from C9 to C35 saturates. The aromatics included mostly alkyl derivatives of xylene, benzene, and phenanthrene. The oxygenated compounds were mostly saturated alcohols, carboxylates, and esters, whereas the major naphthenic compounds included alkylated cyclopentane and cyclohexane. The HCs identified in the refinery wastewater sample agree with the literature reports [5,63]. The GCMS spectra of the refinery wastewater treated by adsorption over AC show no major peaks, except for the solvent peak (used for extraction) with a peak area of about 99.6%, whereas none of the parent HCs are present in the sample. This shows that AC efficiently removed all HCs from the wastewater in 105 min. These results are endorsed by the percentage removal of HCs in the model wastewater and the decrease in the COD of the refinery wastewater. The GC-MS chromatogram of the refinery wastewater treated by photocatalytic oxidation also does not show the presence of any peak corresponding to parent HCs, which suggests that the HCs in the sample were degraded

by oxidation [9]. However, some minor peaks can be observed in the chromatogram, which shows the presence of oxygenated HCs with a relative percentage concentration smaller than 0.02%. These compounds were identified to be octa-decatrienoic acid, hexadecanol, nonadecatriene-diol, pentadecanoic acid, methyl-methyl ester, and hepta-triacotanol. It can be assumed that some of the parent HCs were not completely degraded during photocatalytic oxidation; rather, they were partially oxidized to give the oxygenated byproducts, due to their resilient nature [40].

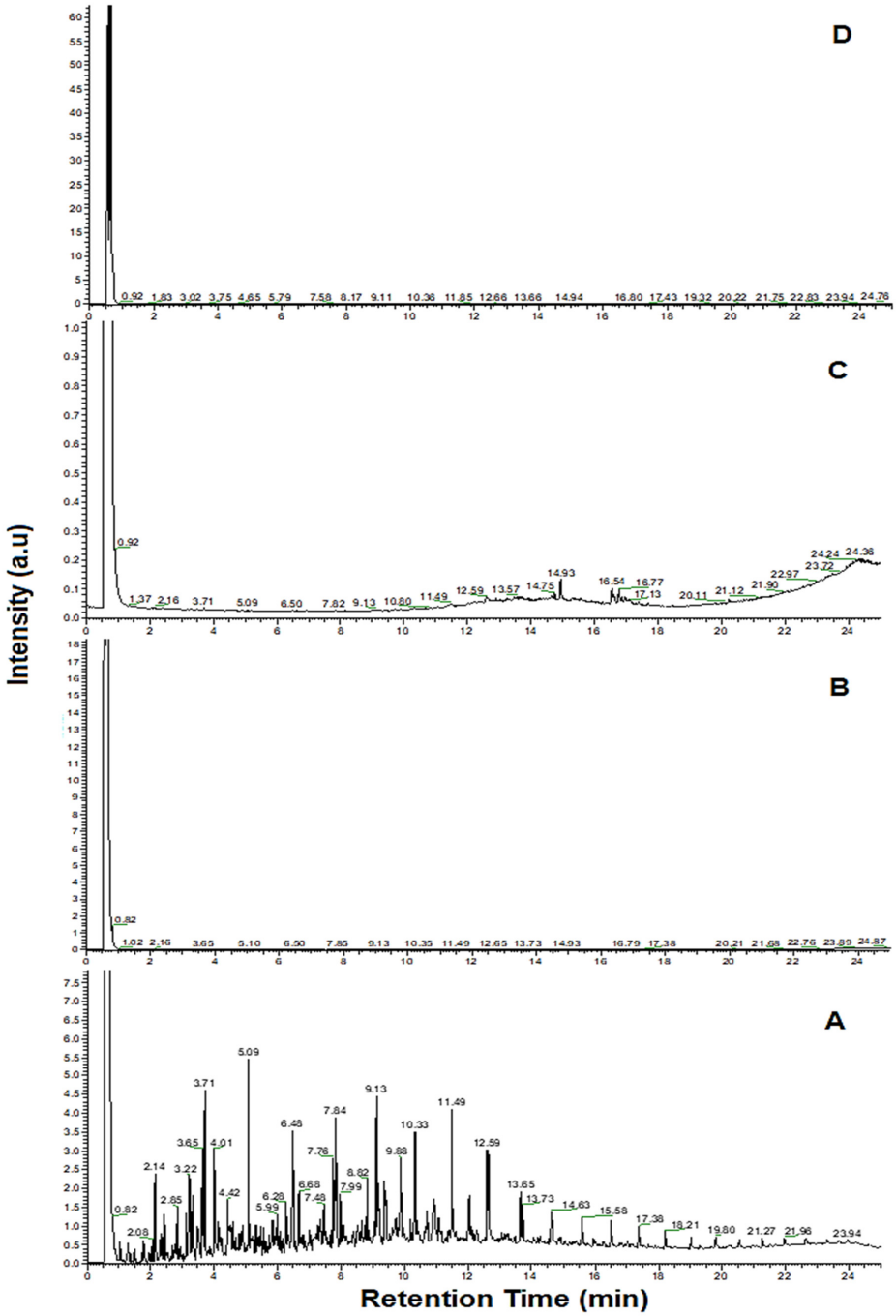

Figure 9. GC-MS chromatograms of (**A**) refinery wastewater sample, refinery wastewater treated by (**B**) adsorption over AC, (**C**) photo-oxidation by UV/TiO_2, (**D**) integrated photo-oxidation and adsorption over TiO_2/AC.

The GC-MS analysis of the refinery wastewater sample treated by integrated photocatalytic oxidation and adsorption over TiO_2/AC shows that all the parent HCs were removed,

and none of the oxidation byproducts were left in the sample. Although the removal of HCs also occurred in case of adsorption over AC, it took about 105 min. Likewise, photocatalytic oxidation removed more than 90% of HCs in 90 min, but some oxidation byproducts were left behind. On the other hand, in the case of the integrated treatment process, the dual effect of oxidation and adsorption almost completely removed all the HCs in just 50 min.

2.9. Process Mechanism

In the integrated photocatalytic oxidation and adsorption process using TiO_2/AC, the removal of HCs occurs in two pathways i.e., photo-oxidation and adsorption, by virtue of the bifunctionality of the hybrid catalyst/adsorbent. The TiO_2 functionality catalyzes the photocatalytic oxidation of HCs under UV irradiation, during which susceptible compounds are completely oxidized [9,63], whereas the resistant HCs are partially oxidized. These resilient HCs as well as the oxidation byproducts are adsorbed over the AC. This phenomenon is supported by the results of the GC-MS analysis.

The mechanism of the photodegradation of organic pollutants by TiO_2 in the presence of UV light has been extensively explained [9]. The illumination of TiO_2 by UV radiation with energy equivalent to its band gap causes the excitation of electrons from the valance band to the conduction band, and an electron hole in the valence band is created. The free electrons in the conduction band and the holes in the valence band become involved in the redox reactions with the substrate on the surface of the catalysts [64]. At the valance band gap (h_{vb}^{+}) with +ive potential, the water molecule on the catalyst surface is split to produce OH· radicals, whereas the electrons in the (e_{CB}^{-}) conduction band convert O_2 on the surface to excited O_2^{-}·, and this in turn leads to the production of an OH· radical [65–67]. The OH· radical, being a strong oxidizing agent, degrades the HCs to CO_2 and H_2O.

The role of AC in TiO_2/AC is the adsorption of aromatic, aliphatic, and partially oxidized HCs. AC is a favorite medium for the adsorption of various organic and inorganic impurities due to its high surface area, nonpolar character, and porous structure, which adsorbs the organic compounds through several mechanisms, including hydrogen bonding, the formation of a donor accepter complex, π–π interaction, etc. [68]. Commonly, the adsorption of HCs is attributed to the number and type of oxygenated functional groups at the surface of AC, which facilitates the HC adsorption via hydrogen bonding. These functionalities also influence the delocalization of the electron and control surface charge. The π–π interaction between the delocalized π electrons of aromatic HC and the π electrons of the graphite ring on the surface of the AC also cause the binding of aromatics on AC [69]. Likewise, the aromatic ring may act as an electron acceptor and the surface carboxylic acid group of AC as an electron donor, which establishes an acceptor–donor complex, resulting in adsorption [70]. Hence, multiple types of interactions are involved in the adsorption of HCs over the AC. This is described in a previous section, i.e., the adsorption of HCs over AC follows both the Langmuir and Freundlich adsorption isotherms, which suggests that the adsorption of HCs occurs in both ways—as monolayer on the surface, as well as in the pores as heterogeneous adsorption—or it may also be assumed that different HC molecules may behave differently. The mechanism of removal of the HCs may be graphically presented, as in Scheme 1 below.

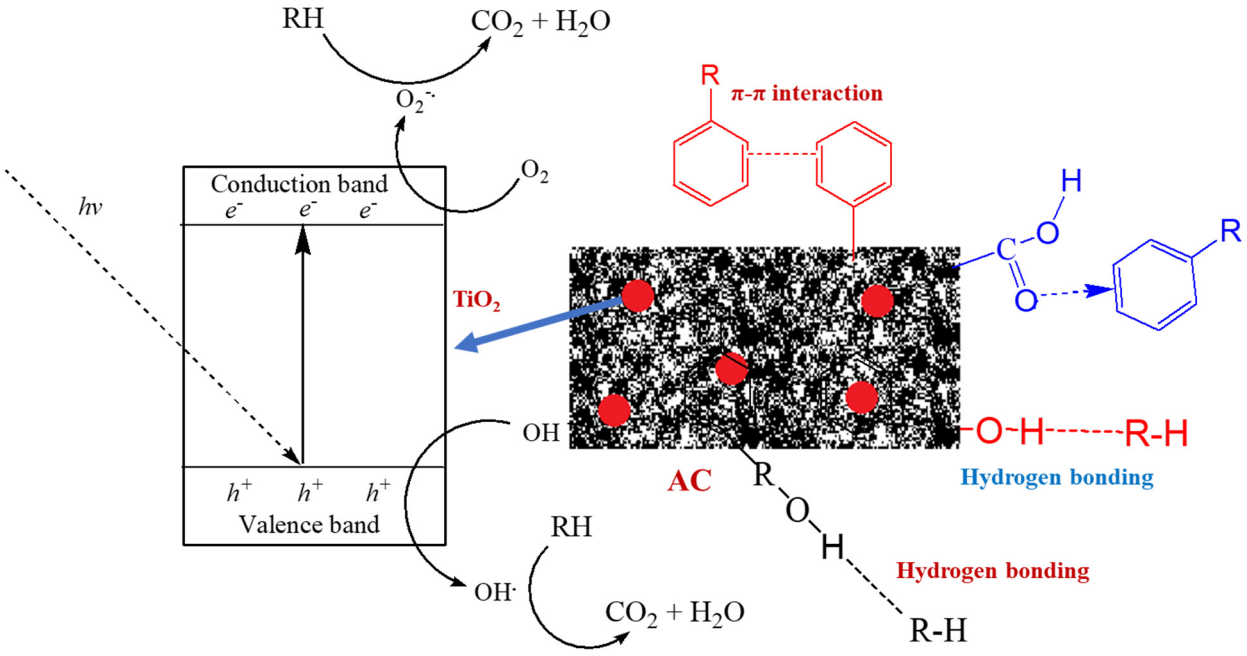

Scheme 1. Mechanism of oxidation and adsorption.

3. Materials and Methods

3.1. Reagents and Chemicals

All the regents and chemicals used in this study were of analytical grade and utilized without any further purification unless mentioned. Model HCs used were (99%) (Fischer Scientific, (Leicestershire, UK). Model wastewater was prepared by dissolving benzene, toluene, phenol, and naphthalene (model HCs) in distilled water with a concentration of 100 mg/L of each. The activated carbon (AC) was purchased from Duksan Chemicals (Siheung-si, Korea); the BET surface area of the AC was about 3000 m^2/g. Refinery wastewater samples were collected from Attock Oil Refinery Ltd., Morgah Rawalpindi, Pakistan. Samples were collected from the point at which the wastewater leaves the dissolved air flotation (DAF) unit. Samples were collected in glass bottles, transported to the laboratory, and stored in the refrigerator to avoid the loss and decomposition of HCs. The samples were characterized by preliminary characterization, such as of the COD, pH, electrical conductivity, total suspended solids, turbidity, and density, which were analyzed through the standard methods.

3.2. Preparation and Characterization of TiO_2/AC Hybrid Adsorbent

TiO_2 supported on an AC hybrid adsorbent was prepared by a low-temperature impregnation method [44]. About 50 mL of methanol was taken in a beaker, to which 0.09 mL of titanium tetraethoxide ($Ti(OC_2H_5)_4$) was added with the help of a micro pipette under ominous stirring until complete dissolution. About 400 mg of AC was added to it and further stirred for 1 h to homogenize the dispersion. The suspension was then filtered through a filter paper, and the residue was dried in oven at 90 °C for about 3 h. The dried solid product was then calcined in a furnace at 400 °C under a nitrogen atmosphere to obtain TiO_2-loaded AC (TiO_2/AC).

3.3. Characterization of TiO_2/AC

The TiO_2/AC prepared in the laboratory was characterized by SEM, EDX, XRD, and FTIR analysis. FTIR analysis of the samples was carried out by a FTIR spectrophotometer (Perkin Elmer, Spectrum II, Waltham, MA, USA), integrated with an ATR sample base diamond plate. The spectra of the samples were recorded at a resolution 4 cm^{-1} and in a scan range of 4000 to 450 cm^{-1} by NTOS2 software. The surface morphology of the

materials was analyzed by scanning electron microscope (Hitachi S-4700, Tokyo, Japan). The elemental analysis of the materials was carried out by energy-dispersive X-ray analysis, through an X-ray source equipped with SEM. XRD analysis of the materials was performed using an X-ray diffractometer (Xpert Philips, Almelo, Netherlands). The source of radiation of the X-ray diffractometer was CuKα, and λ = 1.54 Å was the radiation wavelength. The diffraction patterns of the powder samples were recorded at an angle range of 10 to 80 degrees.

3.4. Adsorption Experiments

The adsorption experiments were carried out in batch mode. About 100 mL of model wastewater was taken in a conical flask, a known amount of AC was added to it, and it was stirred on a magnetic stirrer for a certain time. The adsorbent was recovered by filtration, and the concentration of HCs removed was analyzed through HPLC. The adsorption experiments were carried out under variable conditions of temperature, time, and adsorbent dose. The adsorption data were interpreted through kinetics and isotherm models, and the thermodynamic parameters were also evaluated. Using the same procedure, the treatment of refinery wastewater was also carried out similarly, and the decrease in the HCs' concentration was monitored through COD analysis.

3.5. Integrated Photocatalytic Oxidation-Adsorption Experiments

In integrated photocatalytic oxidation and adsorption experiments, about 500 mL of model wastewater was charged into the photoreactor (Figure 10), and a known weight of TiO_2/AC was added to it. The sample was photo-irradiated by UV lamp under continuous stirring for about 120 min. The UV lamp used was mercury 400W (200–550 nm), having the highest irradiation peak at 365 nm. The sample was filtered, and the concentration of HCs was analyzed through HPLC. The reaction was carried out under different conditions of TiO_2/AC dosage, temperature, and reaction time. The treatment of the real refinery wastewater was also carried out following the same procedure, and the HC content was monitored via COD analysis.

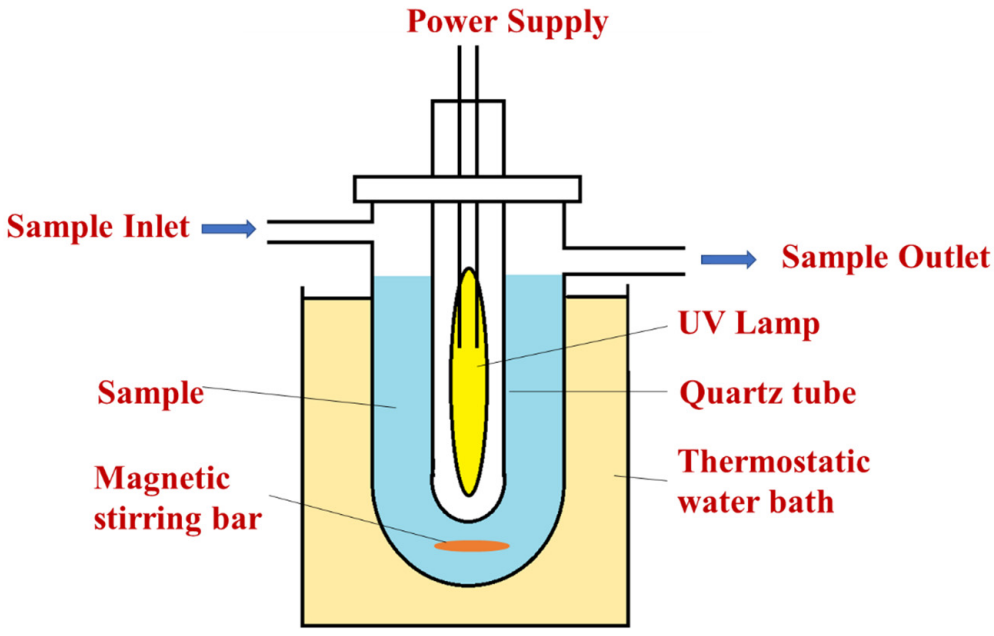

Figure 10. Design of the photoreactor.

3.6. Sample Analyses

In model wastewater, the concentrations of benzene, toluene, phenol, and naphthalene were analyzed by HPLC (Shimadzu, Kyoto, Japan) equipped with a C18 column, using

acetonitrile and deionized water (60:40) as a solvent system, for 10 min run time at a wavelength of 254 nm. A calibration curve was plotted from the peak areas of different standard concentrations of model HCs, from which the concentrations of HCs in the sample were measured. The decrease in the concentration of HCs at time t (C_t mg/L) from the initial concentration (C_o mg/L) was calculated as the percentage removal of model HCs, using Equation (1):

$$\% \text{ removal of HCs } = \frac{Co - Ct}{Co} \times 100 \quad (1)$$

The concentration of HC pollutants in the real refinery wastewater was determined as chemical oxygen demand, which was analyzed through the standard method reported in the literature [40].

Individual HC compounds in the refinery wastewater were identified through GC-MS analysis (Thermo Scientific (DSQ II) GC-MS, Waltham, MA, USA), furnished with a TR-SMS capillary column (30 m × 0.25 µm × 0.25 mm i.d). The flow rate of He, as a carrier gas, was 1 mL/min. The sample injection volume was 1 µL, and the initial oven temperature was 50 °C, with 1 min hold, then raised to 280 °C with a ramp of 6 °C/min and hold for 1 min. The chromatograms were interpreted by matching with individual HCs with the data in the MAINLIB and Replib libraries.

4. Conclusions

In summary, the removal of HC pollutants from refinery wastewater was investigated by integrated photocatalytic oxidation and adsorption over TiO_2/AC prepared in the laboratory. Adsorption over AC resulted in more than 90% removal of model HCs from model wastewater, under an AC dose of 0.6 g, 35 °C in 105 min. The adsorption of HCs by AC followed the pseudo-first-order kinetic model. The adsorption data were best fit to both the Langmuir and Freundlich isotherms. Under optimized conditions, the reduction in the COD of refinery wastewater by adsorption over AC was found to be 92%. Integrated oxidation and adsorption of the model wastewater in the presence of TiO_2/AC led to about 90% removal of all HCs in 50 min at pH 3, 30 °C, and a dose of 250 mg for 100 mL of sample. In the case of the refinery wastewater, TiO_2/AC removed about 95% COD under UV irradiation at optimized conditions. The integrated process brings about more than the same level of decrease in the COD of the refinery wastewater in just 50 min, which is attained by adsorption over AC in 120 min and photocatalytic oxidation using the UV/TiO_2 system in 90 min. The GCMS analysis indicated that in the case of the integrated process treatment, no traces of HCs were left in the treated refinery wastewater sample. This technology can also be applied for other streams containing various types of organic pollutants.

Supplementary Materials: The following supporting information can be downloaded at: https://www.mdpi.com/article/10.3390/catal13010193/s1, Figure S1. EDX profile of TiO_2/AC; Figure S2. First order kinetic plots for adsorption of (a) benzene (b) toluene (c) phenol and (d) naphthalene over activated carbon; Figure S3. Second order kinetic plots for adsorption of (a) benzene (b) toluene (c) phenol and (d) naphthalene over activated carbon. Figure S4. Langmuir isotherms for Benzene (a), Toluene (b), Phenol (c) and Naphthalene (d) adsorption over activated carbon; Figure S5. Freundlich isotherms for Benzene (a), Toluene (b), Phenol (c) and Naphthalene (d) adsorption over activated carbon; Table S1. Physiochemical characteristics of refinery wastewater collected from ARL; Table S2. Hydrocarbons identified by GC-MS analysis in untreated and treated refinery wastewater sample [38,71,72].

Author Contributions: Conceptualization, supervision, project administration, funding acquisition, W.A. and I.A.; investigation, methodology, formal analysis, writing—original draft preparation, I.U.H., W.A. and T.M.; writing—review and editing, visualization, M.Y. and A.S. All authors have read and agreed to the published version of the manuscript.

Funding: This research was funded by the Higher Education Commission of Pakistan under the NRPU program (grant no. NRPU-9056).

Data Availability Statement: Not applicable.

Acknowledgments: The authors acknowledge the financial support for this study from the Higher Education Commission of Pakistan. The authors also acknowledge the cooperation of Attock Oil Refinery Ltd., Morgah, Rawalpindi, for providing the wastewater samples for this study.

Conflicts of Interest: The authors declare no conflict of interest.

References

1. Suleĭmanov, R.; Gabbasova, I.; Sitdikov, R. Changes in the properties of oily gray forest soil during biological reclamation. *Izv. Akad. Nauk. Seriia Biol.* **2005**, *32*, 109–115. [CrossRef]
2. Wake, H. Oil refineries: A review of their ecological impacts on the aquatic environment. *Estuar. Coast. Shelf Sci.* **2005**, *62*, 131–140. [CrossRef]
3. Wang, R.; Liu, J.; Gao, F.; Zhou, J.; Cen, K. The slurrying properties of slurry fuels made of petroleum coke and petrochemical sludge. *Fuel Process. Technol.* **2012**, *104*, 57–66. [CrossRef]
4. Ye, G.; Lu, X.; Han, P.; Peng, F.; Wang, Y.; Shen, X. Application of ultrasound on crude oil pretreatment. *Chem. Eng. Process. Process Intensif.* **2008**, *47*, 2346–2350. [CrossRef]
5. Stepnowski, P.; Siedlecka, E.; Behrend, P.; Jastorff, B. Enhanced photo-degradation of contaminants in petroleum refinery wastewater. *Water Res.* **2002**, *36*, 2167–2172. [CrossRef]
6. Coelho, A.; Castro, A.V.; Dezotti, M.; Sant'Anna Jr, G. Treatment of petroleum refinery sourwater by advanced oxidation processes. *J. Hazard. Mater.* **2006**, *137*, 178–184. [CrossRef] [PubMed]
7. El-Naas, M.H.; Alhaija, M.A.; Al-Zuhair, S. Evaluation of a three-step process for the treatment of petroleum refinery wastewater. *J. Environ. Chem. Eng.* **2014**, *2*, 56–62. [CrossRef]
8. *World Energy Outlook 2019*; IEA (International Energy Agency): Paris, France, 2019.
9. Saien, J.; Nejati, H. Enhanced photocatalytic degradation of pollutants in petroleum refinery wastewater under mild conditions. *J. Hazard. Mater.* **2007**, *148*, 491–495. [CrossRef] [PubMed]
10. Shinde, D.R.; Tambade, P.S.; Chaskar, M.G.; Gadave, K.M. Photocatalytic degradation of dyes in water by analytical reagent grades ZnO, TiO_2 and SnO_2: A comparative study. *Drink. Water Eng. Sci.* **2017**, *10*, 109–117. [CrossRef]
11. El-Naas, M.H.; Surkatti, R.; Al-Zuhair, S. Petroleum refinery wastewater treatment: A pilot scale study. *J. Water Process. Eng.* **2016**, *14*, 71–76. [CrossRef]
12. Mahjoubi, F.Z.; Khalidi, A.; Abdennouri, M.; Barka, N. Zn–Al layered double hydroxides intercalated with carbonate, nitrate, chloride and sulphate ions: Synthesis, characterisation and dye removal properties. *J. Taibah Univ. Sci.* **2017**, *11*, 90–100. [CrossRef]
13. Guo, S.; Zhang, L.; Chen, M.; Ahmad, F.; Fida, H.; Zhang, H. Heterogeneous Activation of Peroxymonosulfate by a Spinel $CoAl_2O_4$ Catalyst for the Degradation of Organic Pollutants. *Catalysts* **2022**, *12*, 847. [CrossRef]
14. Lv, N.; Wang, X.; Peng, S.; Zhang, H.; Luo, L. Study of the kinetics and equilibrium of the adsorption of oils onto hydrophobic jute fiber modified via the sol-gel method. *Int. J. Environ. Res. Public Health.* **2018**, *15*, 969. [CrossRef] [PubMed]
15. Channa, A.M.; Baytak, S.; Memon, S.Q.; Talpur, M.Y. Equilibrium, kinetic and thermodynamic studies of removal of phenol from aqueous solution using surface engineered chemistry. *Heliyon* **2019**, *5*, e01852. [CrossRef] [PubMed]
16. Kumar, K.V.; de Castro, M.M.; Martinez-Escandell, M.; Molina-Sabio, M.; Rodriguez-Reinoso, F. A continuous binding site affinity distribution function from the Freundlich isotherm for the supercritical adsorption of hydrogen on activated carbon. *J. Phys. Chem. C* **2010**, *114*, 13759–13765. [CrossRef]
17. Ghaedi, M.; Nasab, A.G.; Khodadoust, S.; Rajabi, M.; Azizian, S. Application of activated carbon as adsorbents for efficient removal of methylene blue: Kinetics and equilibrium study. *J. Ind. Eng. Chem.* **2014**, *20*, 2317–2324. [CrossRef]
18. Rathee, G.; Awasthi, A.; Sood, D.; Tomar, R.; Tomar, V.; Chandra, R. A new biocompatible ternary Layered Double Hydroxide Adsorbent for ultrafast removal of anionic organic dyes. *Sci. Rep.* **2019**, *9*, 16225. [CrossRef]
19. Ghaedi, M.; Mazaheri, H.; Khodadoust, S.; Hajati, S.; Purkait, M. Application of central composite design for simultaneous removal of methylene blue and Pb^{2+} ions by walnut wood activated carbon. *Spectrochim. Acta—A Mol. Biomol.* **2015**, *135*, 479–490. [CrossRef]
20. Delaune, R.; Lindau, C.; Jugsujinda, A. Effectiveness of "Nochar" solidifier polymer in removing oil from open water in coastal wetlands. *Spill Sci. Technol. Bull.* **1999**, *5*, 357–359. [CrossRef]
21. Pelletier, É.; Siron, R. Silicone-based polymers as oil spill treatment agents. *Environ. Toxicol. Chem.* **1999**, *18*, 813–818. [CrossRef]
22. Lim, T.-T.; Huang, X. Evaluation of kapok (*Ceiba pentandra* (L.) Gaertn.) as a natural hollow hydrophobic–oleophilic fibrous sorbent for oil spill cleanup. *Chemosphere* **2007**, *66*, 955–963. [CrossRef] [PubMed]
23. Pham, V.T.; Nguyen, H.-T.T.; Thi Cam Nguyen, D.; TN Le, H.; Thi Nguyen, T.; Thi Hong Le, N.; Lim, K.T.; Duy Nguyen, T.; Tran, T.V.; Bach, L.G. Process Optimization by a Response Surface Methodology for Adsorption of Congo Red Dye onto Exfoliated Graphite-Decorated $MnFe_2O_4$ Nanocomposite: The Pivotal Role of Surface Chemistry. *Processes* **2019**, *7*, 305. [CrossRef]
24. Lupandina, N.; Sapronova, Z.A. Modified Bleaching Clay as a Sorption Material. *E&ES* **2020**, *459*, 042063.
25. Pereira, K.R.d.O.; Hanna, R.A.; Vianna, M.M.G.R.; Pinto, C.A.; Rodrigues, M.G.F.; Valenzuela-Diaz, F.R. Brazilian organoclays as nanostructured sorbents of petroleum-derived hydrocarbons. *Mater. Res.* **2005**, *8*, 77–80. [CrossRef]
26. Giusti, D.; Conway, R.; Lawson, C. Activated carbon adsorption of petrochemicals. *J. Water Pollut. Control. Fed.* **1974**, *46*, 947–965.

27. Abussaud, B.; Asmaly, H.A.; Saleh, T.A.; Gupta, V.K.; Atieh, M.A. Sorption of phenol from waters on activated carbon impregnated with iron oxide, aluminum oxide and titanium oxide. *J. Mol. Liq.* **2016**, *213*, 351–359. [CrossRef]
28. Tong, K.; Zhang, Y.; Fu, D.; Meng, X.; An, Q.; Chu, P.K. Removal of organic pollutants from super heavy oil wastewater by lignite activated coke. *Colloids. Surf. A Physicochem. Eng. Asp.* **2014**, *447*, 120–130. [CrossRef]
29. Okiel, K.; El-Sayed, M.; El-Kady, M.Y. Treatment of oil–water emulsions by adsorption onto activated carbon, bentonite and deposited carbon. *Egypt. J. Pet.* **2011**, *20*, 9–15. [CrossRef]
30. Alhakimi, G.; Studnicki, L.H.; Al-Ghazali, M. Photocatalytic destruction of potassium hydrogen phthalate using TiO_2 and sunlight: Application for the treatment of industrial wastewater. *J. Photochem. Photobiol. A Chem.* **2003**, *154*, 219–228. [CrossRef]
31. Guo, S.; Yang, Z.; Zhang, H.; Yang, W.; Li, J.; Zhou, K. Enhanced photocatalytic degradation of organic contaminants over $CaFe_2O_4$ under visible LED light irradiation mediated by peroxymonosulfate. *J. Mater. Sci. Technol.* **2021**, *62*, 34–43. [CrossRef]
32. Haarstrick, A.; Kut, O.M.; Heinzle, E. TiO_2-assisted degradation of environmentally relevant organic compounds in wastewater using a novel fluidized bed photoreactor. *Environ. Sci. Technol.* **1996**, *30*, 817–824. [CrossRef]
33. Bahnemann, D.; Kholuiskaya, S.; Dillert, R.; Kulak, A.; Kokorin, A. Photodestruction of dichloroacetic acid catalyzed by nano-sized TiO_2 particles. *Appl. Catal. B* **2002**, *36*, 161–169. [CrossRef]
34. Chen, J.; Liu, M.; Zhang, L.; Zhang, J.; Jin, L. Application of nano TiO_2 towards polluted water treatment combined with electro-photochemical method. *Water Res.* **2003**, *37*, 3815–3820. [CrossRef] [PubMed]
35. Ani, I.J.; Akpan, U.G.; Olutoye, M.A.; Hameed, B.H. Photocatalytic degradation of pollutants in petroleum refinery wastewater by TiO_2- and ZnO-based photocatalysts: Recent development. *J. Clean. Prod.* **2018**, *205*, 930–954. [CrossRef]
36. Abdelwahab, O.; Amin, N.; El-Ashtoukhy, E.Z. Electrochemical removal of phenol from oil refinery wastewater. *J. Hazard. Mater.* **2009**, *163*, 711–716. [CrossRef]
37. Lin, L.; Jiang, W.; Chen, L.; Xu, P.; Wang, H. Treatment of produced water with photocatalysis: Recent advances, affecting factors and future research prospects. *Catalysts* **2020**, *10*, 924. [CrossRef]
38. Santos, F.; Azevedo, E.; Dezotti, M. Photocatalysis as a tertiary treatment for petroleum refinery wastewaters. *Braz. J. Chem. Eng.* **2006**, *23*, 451–460. [CrossRef]
39. Li, J.; Song, X.; Hu, G.; Thring, R.W. Ultrasonic desorption of petroleum hydrocarbons from crude oil contaminated soils. *J. Environ. Sci. Health A* **2013**, *48*, 1378–1389. [CrossRef] [PubMed]
40. Ul haq, I.; Ahmad, W.; Ahmad, I.; Yaseen, M. Photocatalytic oxidative degradation of hydrocarbon pollutants in refinery wastewater using TiO_2 as catalyst. *Water Environ. Res.* **2020**, *92*, 2086–2094. [CrossRef] [PubMed]
41. Đukić, A.B.; Kumrić, K.R.; Vukelić, N.S.; Stojanović, Z.S.; Stojmenović, M.D.; Milošević, S.S.; Matović, L.L. Influence of ageing of milled clay and its composite with TiO_2 on the heavy metal adsorption characteristics. *Ceram. Int.* **2015**, *41*, 5129–5137. [CrossRef]
42. Zhu, Z.-l.; Li, A.-m.; Xia, M.-f.; Wan, J.-n.; Zhang, Q.-x. Preparation and characterization of polymer-based spherical activated carbons. *Chin. J. Polym. Sci.* **2008**, *26*, 645–651. [CrossRef]
43. Thamaphat, K.; Limsuwan, P.; Ngotawornchai, B. Phase characterization of TiO_2 powder by XRD and TEM. *Kasetsart J. Nat. Sci.* **2008**, *42*, 357–361.
44. Huang, D.; Miyamoto, Y.; Matsumoto, T.; Tojo, T.; Fan, T.; Ding, J.; Guo, Q.; Zhang, D. Preparation and characterization of high-surface-area TiO_2/activated carbon by low-temperature impregnation. *Sep. Purif. Technol.* **2011**, *78*, 9–15. [CrossRef]
45. Olafadehan, O.; Aribike, D. Treatment of industrial wastewater effluent. *J. Niger. Soc. Chem. Eng.* **2000**, *19*, 50–53.
46. Daud, W.M.A.W.; Houshamnd, A.H. Textural characteristics, surface chemistry and oxidation of activated carbon. *J. Nat. Gas Chem.* **2010**, *19*, 267–279. [CrossRef]
47. Abbaszadeh, S.; Wan Alwi, S.R.; Webb, C.; Ghasemi, N.; Muhamad, I.I. Treatment of lead-contaminated water using activated carbon adsorbent from locally available papaya peel biowaste. *J. Clean. Prod.* **2016**, *118*, 210–222. [CrossRef]
48. Gupta, V.K.; Gupta, B.; Rastogi, A.; Agarwal, S.; Nayak, A. A comparative investigation on adsorption performances of mesoporous activated carbon prepared from waste rubber tire and activated carbon for a hazardous azo dye—Acid Blue 113. *J. Hazard. Mater.* **2011**, *186*, 891–901. [CrossRef] [PubMed]
49. Mohammed, J.; Nasri, N.S.; Zaini, M.A.A.; Hamza, U.D.; Ani, F.N. Adsorption of benzene and toluene onto KOH activated coconut shell based carbon treated with NH3. *Int. Biodeterior. Biodegrad.* **2015**, *102*, 245–255. [CrossRef]
50. Kilic, M.; Apaydin-Varol, E.; Pütün, A.E. Adsorptive removal of phenol from aqueous solutions on activated carbon prepared from tobacco residues: Equilibrium, kinetics and thermodynamics. *J. Hazard. Mater.* **2011**, *189*, 397–403. [CrossRef] [PubMed]
51. Ayawei, N.; Ebelegi, A.N.; Wankasi, D. Modelling and interpretation of adsorption isotherms. *J. Chem.* **2017**, *2017*, 3039817. [CrossRef]
52. Mittal, A.; Kurup, L.; Mittal, J. Freundlich and Langmuir adsorption isotherms and kinetics for the removal of Tartrazine from aqueous solutions using hen feathers. *J. Hazard. Mater.* **2007**, *146*, 243–248. [CrossRef] [PubMed]
53. Liu, H.; Dong, Y.; Wang, H.; Liu, Y. Adsorption behavior of ammonium by a bioadsorbent–Boston ivy leaf powder. *Res. J. Environ. Sci.* **2010**, *22*, 1513–1518. [CrossRef]
54. Desta, M.B. Batch sorption experiments: Langmuir and Freundlich isotherm studies for the adsorption of textile metal ions onto teff straw (*Eragrostis tef*) agricultural waste. *J. Thermodyn.* **2013**, *2013*, 375830. [CrossRef]
55. Kim, K.-J.; Kang, C.-S.; You, Y.-J.; Chung, M.-C.; Woo, M.-W.; Jeong, W.-J.; Park, N.-C.; Ahn, H.-G. Adsorption–desorption characteristics of VOCs over impregnated activated carbons. *Catal. Today* **2006**, *111*, 223–228. [CrossRef]

56. Rodrigues, L.A.; da Silva, M.L.C.P.; Alvarez-Mendes, M.O.; dos Reis Coutinho, A.; Thim, G.P. Phenol removal from aqueous solution by activated carbon produced from avocado kernel seeds. *Chem. Eng. J.* **2011**, *174*, 49–57. [CrossRef]
57. Tham, Y.; Latif, P.A.; Abdullah, A.; Shamala-Devi, A.; Taufiq-Yap, Y. Performances of toluene removal by activated carbon derived from durian shell. *Bioresour. Technol.* **2011**, *102*, 724–728. [CrossRef] [PubMed]
58. Alkaram, U.F.; Mukhlis, A.A.; Al-Dujaili, A.H. The removal of phenol from aqueous solutions by adsorption using surfactant-modified bentonite and kaolinite. *J. Hazard. Mater.* **2009**, *169*, 324–332. [CrossRef]
59. Brandão, P.C.; Souza, T.C.; Ferreira, C.A.; Hori, C.E.; Romanielo, L.L. Removal of petroleum hydrocarbons from aqueous solution using sugarcane bagasse as adsorbent. *J. Hazard. Mater.* **2010**, *175*, 1106–1112. [CrossRef]
60. Greenberg, A.E.; Clesceri, L.S.; Eaton, A.D. *Standard Methods for the Examination of Water and Wastewater*; American Public Health Association: Washington, DC, USA, 1992.
61. El-Gawad, S.; El-Aziz, H. Effective removal of chemical oxygen demand and phosphates from aqueous medium using entrapped activated carbon in alginate. *MOJ Biol. Med.* **2018**, *3*, 227–236. [CrossRef]
62. Sun, W.-l.; Qu, Y.-z.; Yu, Q.; Ni, J.-r. Adsorption of organic pollutants from coking and papermaking wastewaters by bottom ash. *J. Hazard. Mater.* **2008**, *154*, 595–601. [CrossRef]
63. Saien, J.; Shahrezaei, F. Organic pollutants removal from petroleum refinery wastewater with nanotitania photocatalyst and UV light emission. *Int. J. Photoenergy* **2012**, *2012*, 703074. [CrossRef]
64. Pakravan, P.; Akhbari, A.; Moradi, H.; Azandaryani, A.H.; Mansouri, A.M.; Safari, M. Process modeling and evaluation of petroleum refinery wastewater treatment through response surface methodology and artificial neural network in a photocatalytic reactor using poly ethyleneimine (PEI)/titania (TiO_2) multilayer film on quartz tube. *Appl. Petrochem. Res.* **2015**, *5*, 47–59. [CrossRef]
65. Bickley, R.; Slater, M.; Wang, W.-J. Engineering development of a photocatalytic reactor for waste water treatment. *Process. Saf. Environ. Prot.* **2005**, *83*, 205–216. [CrossRef]
66. Masschelein, W.; Rice, R. *Ultraviolet Light in Water and Wastewater Sanitation*; Lewis Publishers: Boca Raton, FL, USA, 2002; pp. 3–4.
67. Saien, J.; Soleymani, A. Degradation and mineralization of Direct Blue 71 in a circulating upflow reactor by UV/TiO_2 process and employing a new method in kinetic study. *J. Hazard. Mater.* **2007**, *144*, 506–512. [CrossRef]
68. Benyahia, F.; Abdulkarim, M.; Embaby, A.; Rao, M. Refinery wastewater treatment: A true technological challenge. In Proceedings of the Seventh Annual UAE University Research Conference, Al-Ain, United Arab Emirates, 22–24 April 2006.
69. da Silva, L.J.; Alves, F.C.; de França, F.P. A review of the technological solutions for the treatment of oily sludges from petroleum refineries. *Waste Manag. Res.* **2012**, *30*, 1016–1030. [CrossRef] [PubMed]
70. Bernal, V.; Giraldo, L.; Moreno-Piraján, J.C.; Balsamo, M.; Erto, A. Mechanisms of Methylparaben Adsorption onto Activated Carbons: Removal Tests Supported by a Calorimetric Study of the Adsorbent-Adsorbate Interactions. *Molecules* **2019**, *24*, 413. [CrossRef]
71. Hami, M.L.; Al-Hashimi, M.; Al-Doori, M. Effect of activated carbon on BOD and COD removal in a dissolved air flotation unit treating refinery wastewater. *Desalination* **2007**, *216*, 116–122. [CrossRef]
72. Ma, F.; Guo, J.B.; Zhao, L.J.; Chang, C.C.; Cui, D. Application of bioaugmentation to improve the activated sludge system into the contact oxidation system treating petrochemical wastewater. *Bioresour. Technol.* **2009**, *100*, 597–602. [CrossRef] [PubMed]